

Department of Physics, Chemistry and Biology

Master's Thesis

Search for Dark Matter in the Upgraded High Luminosity LHC at CERN

Impact of ATLAS phase II performance on a mono-jet analysis

Sven-Patrik Hallsjö

Thesis work performed at Stockholm University

Linköping, June 4, 2014

LITH-IFM-A-EX--14/2863--SE



**Linköpings universitet
TEKNISKA HÖGSKOLAN**

Department of Physics, Chemistry and Biology
Linköping University
SE-581 83 Linköping, Sweden

Search for Dark Matter in the Upgraded High Luminosity LHC at CERN

Impact of ATLAS phase II performance on a mono-jet analysis

Sven-Patrik Hallsjö

Thesis work performed at Stockholm University

Linköping, June 4, 2014

Supervisor: **Docent Christophe Clément**
 FYSIKUM Stockholm University
Professor Magnus Johansson
 IFM, Linköping University

Examiner: **Professor Magnus Johansson**
 IFM, Linköping University



Avdelning, Institution
Division, Department

Theoretical physics group
Department of Physics, Chemistry and Biology
SE-581 83 Linköping

Datum
Date

2014-06-04

Språk
Language

Svenska/Swedish
 Engelska/English

Rapporttyp
Report category

Licentiatavhandling
 Examensarbete
 C-uppsats
 D-uppsats
 Övrig rapport

ISBN
—
ISRN
LITH-IFM-A-EX--14/2863--SE

Serietitel och serienummer **ISSN**
Title of series, numbering —

URL för elektronisk version

<http://urn.kb.se/resolve?urn=urn:nbn:se:liu:diva-XXXXXX>

Titel Sökandet efter mörk materia i den uppgraderade hög luminositets LHC i CERN
Title Search for Dark Matter in the Upgraded High Luminosity LHC at CERN

Undertitel Påverkan av ATLAS fas II prestanda på en mono-jet analys
Subtitle Impact of ATLAS phase II performance on a mono-jet analysis

Författare Sven-Patrik Hallsjö
Author

Sammanfattning
Abstract

Something as an introduction:

The LHC at CERN is undergoing an upgrade to increase the center of mass energy for the colliding particles which means that new physical processes will be explored. One drawback of this is that it will be harder to isolate unique particle collisions since more and more collisions will occur simultaneously, so called pile-up.

One hope for the upgrade is that WIMP models of dark matter will be detected.

This thesis covers looking at effective operators which try to explain dark matter without adding new theories to the standard model or QFT.

Some results and a slight conclusion.

Nyckelord

Keywords ATLAS, Beyond standard model physics, CERN, Dark matter, Elementary particle physics, High energy physics, something, this is in mythesis.sty

4 Abstract

5 Something as an introduction:

6 The LHC at CERN is undergoing an upgrade to increase the center of mass en-
7 ergy for the colliding particles which means that new physical processes will be
8 explored. One drawback of this is that it will be harder to isolate unique parti-
9 cle collisions since more and more collisions will occur simultaneously, so called
10 pile-up.

11 One hope for the upgrade is that WIMP models of dark matter will be detected.

12 This thesis covers looking at effective operators which try to explain dark matter
13 without adding new theories to the standard model or QFT.

14 Some results and a slight conclusion.

¹⁵ **Acknowledgments**

¹⁶ I wish to dedicate this thesis to my mathematics teacher Ulf Rydmark without
¹⁷ whom I would not have studied physics.

¹⁸ A big thank you to my family, fiancée and friends who have supported me through-
¹⁹ out my education. A warm thank you to my friend Joakim Skoog who altered
²⁰ some of the images for me.

²¹ I want to thank my supervisor Christophe Clément and all those who helped me
²² at Stockholm University.

²³ I also want to thank my examiner Magnus Johansson, who always took time to
²⁴ answer any question from and support his students.

²⁵ A special thank you to Professor Irina Yakimenko without whom my master years
²⁶ would have been duller and probably impossible.

²⁷ Finally I want to thank someone someone for proofreading my

Linköping, June 2014
Sven-Patrik Hallsjö

Contents

Notation

1 Introduction

1.1	Research goals	2
1.2	Theoretical Background	3
1.2.1	Quantum mechanics and quantum field theory	3
1.2.2	Nuclear, particle and subatomic particle physics	4
1.2.3	The standard model of particle physics	4
1.2.4	Dark matter	5
1.2.5	Effective field theory	6
1.2.6	Search for WIMPS	8
1.3	Experimental overview	10
1.3.1	LHC	10
1.3.2	ATLAS	11
1.3.3	Coordinate system	12
1.3.4	Reconstructing data	12
1.3.5	Pile-up	13
1.3.6	Mono-jet analysis	13
1.3.7	Phase II high luminosity upgrade	14
1.3.8	Monte Carlo simulation	15

2 Validation of smearing functions

2.1	Smearing functions	18
2.2	Validation	19
2.3	Results	20
2.3.1	Electron and photon	21
2.3.2	Muon	22
2.3.3	Tau	22
2.3.4	Jets	23
2.3.5	Missing Transversal Energy	24
2.4	Expected results	25
2.5	Discussion	27
2.5.1	Smearing independent on pile-up	27

63	2.5.2 Comparison to expected results	27
64	2.6 Conclusion	28
65	3 Evaluating dark matter signals	29
66	3.1 Signal to background ratio	29
67	3.1.1 Selection criteria	30
68	3.1.2 Verifying background data	30
69	3.1.3 Figures of merit	31
70	3.1.4 D5 operators	32
71	3.1.5 Light vector mediator models	32
72	3.1.6 Susy models?	32
73	3.2 Other selection criteria and observables	32
74	3.3 Mitigating the effect of the high luminosity	32
75	3.4 Results	33
76	3.4.1 Limit on M^*	33
77	3.4.2 Effect of pile-up on M^*	33
78	3.4.3 Previous results	34
79	3.4.4 Limit on mediator mass	34
80	3.4.5 Effect of pile-up on mediator mass	34
81	3.5 Discussion	34
82	3.6 Conclusion	34
83	4 Results and Conclusions	35
84	4.1 Validation of smearing functions	35
85	4.2 Signal to background ratio	35
86	4.2.1 Limit on M^*	35
87	4.2.2 Limit on mediator mass	35
88	4.3 Other selection criteria and observables	35
89	4.3.1 Limit on M^*	35
90	4.3.2 Limit on mediator mass	35
91	4.4 Mitigating the effect of the high luminosity	35
92	4.5 Recommendations to mitigate the effect of the high luminosity	35
93	4.6 Suggestions for future research	36
94	A Datasets	39
95	A.1 Background processes	39
96	A.1.1 Validation	39
97	A.1.2 Background to signals	39
98	A.2 D5 signal processes	40
99	A.3 Light vector mediator processes	40
100	Bibliography	45

Notation

NOTATIONS

Notation	Explanation
barn(b)	$1 \text{ barn}(b) = 10^{-24} \text{ cm}^2$
\oplus	$a \oplus b = \sqrt{a^2 + b^2}$, $a \oplus b \oplus c = \sqrt{a^2 + b^2 + c^2}$

ABBREVIATIONS

Abbreviation	Expansion
ATLAS	A large Toroidal LHC ApparatuS
CERN	Organisation européenne pour la recherche nucléaire ¹
CMS	Compact Muon Solenoid
LHC	Large Hadron Collider
RMS	Root Mean Square
SM	the Standard Model of particle physics
WIMP	Weakly Interacting Massive Particle
WIMPS	Weakly Interacting Massive ParticleS
QED	Quantum ElectroDynamics
QFT	Quantum Field Theory
QM	Quantum Mechanics

¹Originally, Conseil Européen pour la Recherche Nucléaire

1

Introduction

107 Discrepancies in measurements of the rotations of galaxies indicate the presence
108 of a large amount of matter which interacts through gravity, though not elec-
109 tromagnetically making it invisible to our telescopes. This matter is commonly
110 referred to as dark matter. Since no known or hypothesised particle in the stan-
111 dard model of particle physics can be used as a candidate for dark matter, this
112 hints at the presence of new physics.

113 At the Organisation Européene pour la Recherche Nucléaire (CERN) focus now
114 lies to discover any evidence of so called weakly interacting massive particles
115 (WIMPS) which may be a candidate for dark matter. It is usually impossible to
116 detect any interaction of dark matter candidates on the subatomic scale, however
117 through looking at proposed interactions, searching for assumed decay channels
118 and by investigating what is invisible to the detectors by using momentum con-
119 servation it is hoped that signs will be found. Though to date, none have been
120 found.

121 Both experiments and current theories now show that higher energies are re-
122 quired at the LHC to be able to see any signs. This is why the LHC and all detectors
123 are undergoing a vast upgrade program [1]. In this thesis focus will be on the last
124 part of the upgrade due for completion in 2023, known as the high luminosity-
125 LHC phase II upgrade; and also on the ATLAS detector. The method used in this
126 thesis focuses on looking at data which emulate conditions at the upgraded LHC.

127 1.1 Research goals

128 This research took place at Stockholm University from January 7th until **when**?
129 During the research period the following tasks were set up and performed/answered:

- 130 • Implement a C++ programme that loops over the collisions inside the signal
131 and background datasets.
- 132 • For each collision retrieve the relevant observables (variables used to extract
133 the signal over the background) and apply "smearing functions" to emulate
134 the effect of the high luminosity on the observables.
- 135 • For both signal and background datasets, compare observables before and
136 after smearing. What observables are the least/most affected?
- 137 • Implement selection criteria that selects the signal collisions efficiently while
138 reduces significantly the background. In a first step the selection criteria
139 should be taken from existing studies.
- 140 • Selection criteria can be evaluated and compared with each other using a
141 figure of merit P , that measures the sensitivity of the experiment to the dark
142 matter signal. Calculate P for the given selection criteria before and after
143 smearing.
- 144 • What is the effect of the high luminosity (smearing) on the value of P ?
- 145 • Investigate other selection criteria and observables, to mitigate the effect of
146 high luminosity. Use P to rank different criteria after smearing.
- 147 • Conclude on the effect of the high luminosity on the sensitivity for dark matter
148 and possible ways to mitigate its effects using alternative observables
149 and selection criteria.

1.2 Theoretical Background

1.2.1 Quantum mechanics and quantum field theory

In the beginning of the 20th century, some physical phenomena could not be explained by classical physics, for example the ultra-violet disaster of any classical model of black-body radiation, and the photoelectric effect [2]. It was these phenomena that led to the formulation of quantum mechanics (QM), where energy transfer is quantized and particles can act as both waves and particles at the same time [3].

Combining QM with classical electromagnetism proved harder than expected, colliding a photon(em-field) and an electron (particle/wave) is quite tricky. This can be seen when trying to calculate the scattering between them both in a QM schema. One idea that came from this was to explain them both in the same framework, field theory. Also, trying to incorporate special relativity into QM suggested a field description where space-time is described using the metric formalism from differential geometry. The culmination of both of these problems is the first part of a Quantum field theory (QFT), Quantum electrodynamics (QED) which with incredible precision explains electromagnetic phenomena including effects from special relativity[4]. It is in this merging that antimatter was theorised, since it is a requirement for the theory to hold. After the discovery of antimatter, the theory was set in stone. Since this the theory has been altered somewhat to explain more and more experimental data. This is discussed more in subsection 1.2.2 and subsection 1.2.3.

To be able to calculate properties in QFT one uses the Lagrangian formalism [5], which gives a governing equation for the different physical processes. In general the Lagrangian used for the Standard model is quite complicated, one can thus focus on one of the different terms corresponding to a specific interaction. This can be done to calculate the so called cross-section for a process, which is related to the probability that that process will occur. A step to simplify the calculations is to use the so called Feynman diagrams, an example of which is given in figure 1.1.

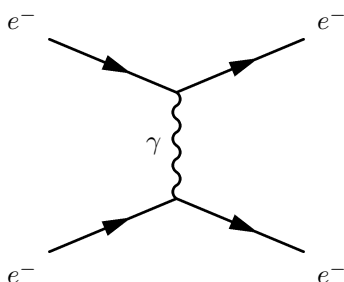


Figure 1.1: An example of a Feynman diagram explaining an electron-electron scattering using QED.

Through the figure, which comes with certain rules, and knowing what the major process (in this case QED) one can calculate the cross-section [4]. It is this that is needed to predict what one will be able to detect new particles.

183 1.2.2 Nuclear, particle and subatomic particle physics

184 Many could argue that these branches of physics started after Ernest Rutherford
 185 famous gold foil experiment [6], where he discovered that matter is composed of
 186 matter with a nucleus, a lot of empty space and electrons.

187 It was this that sparked the curiosity to see what the nucleus is made of and
 188 what forces govern the insides of atoms. After this, and the combination of the
 189 theoretical description given by QM, a lot more has been discovered and still
 190 more has been predicted. The newest of these is of course the Higgs particle,
 191 which was predicted through QFT and then discovered by the ATLAS and the CMS
 192 experiments at CERN [7].

193 The discovered particles are often divided into different groups depending on
 194 the fundamental particles that build them up. For instance, particles build up of
 195 three quarks are known as hadrons. Particles with an integer spin are known as
 196 bosons whereas half-integer particles are known as fermions.

197 1.2.3 The standard model of particle physics

198 The standard model of particle physics, referred to simply as the standard model
 199 (SM), is the particle zoo which tries to categorize all the particles and that have
 200 been discovered experimentally. QFT explains the interactions between these par-
 201 ticles and it has also predicted several particles by including symmetries [6]. Re-
 202 garding SM, Gauge bosons are the force carriers for the different forces, quarks
 203 are the and leptons are the fundamental blocks that we know of so far. The differ-
 ence between the later two is if they interact via the strong force or not.

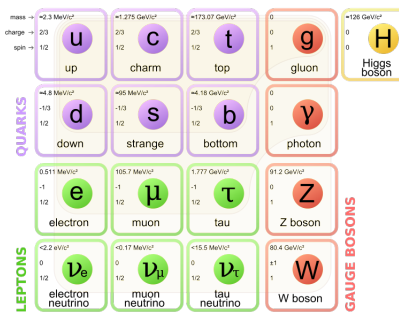


Figure 1.2: The standard model of particle physics where the three first columns represent the so called generations, starting with the first. [8].

204 SM is today the pinnacle of particle physics and can be used to explain almost
 205 everything that occurs around us. There are however some problems [9]:

- 207 • There is no link between gravity and the SM.
- 208 • Asymmetry between matter and antimatter can not be fully explained.
- 209 • No dark matter candidate!
- 210 • No explanation that can contain dark matter.

211 In this thesis focus lies with dark matter, some more introduction to possible
 212 dark matter and different candidates in extensions to SM are explained in subsection
 213 1.2.4.

214 1.2.4 Dark matter

215 Dark matter is among other things, the name given to the solution to the discrepancies
 216 of galactic rotations.

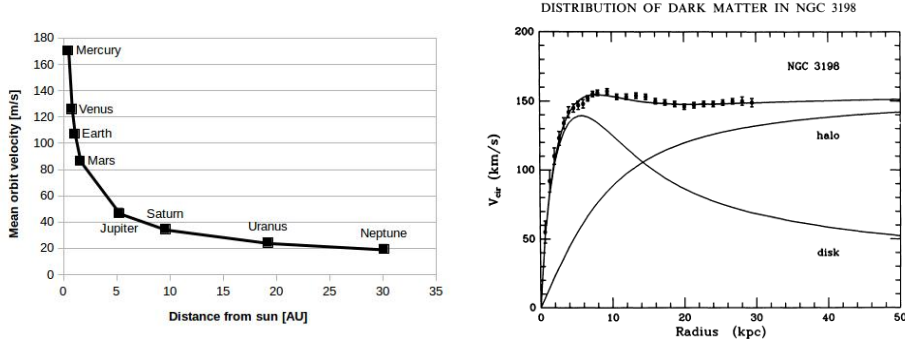
217 To explain this, focus on matter in a galaxy which are rotating around the center
 218 of the galaxy. Through Newtons law of gravity and the centrifugal force one can
 219 calculate the rotation speed dependent on the distance to the center of the galaxy.
 220 Since one of these forces is attractive and the other repulsive, if the matter is in
 221 a stable orbit around the galactic center (which they are) they must be equal and
 222 give us an expression for the speed depending on the distance. Newtons law can
 223 be written as the following:

$$F_{Gravitational} = G \frac{Mm}{r^2} = G_M \frac{m}{r^2} \quad F_{Centrifugal} = m \frac{V^2}{r} \quad (1.1)$$

224 where G is the gravitational constant, M the mass of the centre object, m the mass
 225 of the matter, r the distance between the two and V is the rotation speed. It has
 226 been simplified using G_M since all matter orbits the same galactic center. Setting
 227 the equations in (1.1) results in:

$$G_M \frac{m}{r^2} = m \frac{V^2}{r} \Leftrightarrow V^2 = \frac{G_M}{r} \Rightarrow V = \sqrt{\frac{G_M}{r}} \propto \frac{1}{\sqrt{r}} \quad (1.2)$$

228 where the speed is assumed to be positive and \propto means proportional. Through
 229 these simple calculations it shown that the rotation speed should decrease with
 230 and increased distance. The same reasoning can be applied to our solar system
 231 where this is the case figure 1.3a. The relation in these units is $V = \frac{107}{\sqrt{r}}$ where
 232 107 can be used in (1.2) to calculate the mass of the sun. However when looking
 233 at galaxies, even when taking into account that one has to see the galaxies as a
 234 mass distribution and that the above is only true when outside of the inner mass
 235 half, this is not the case! In figure 1.3b experimental data can be seen from the
 236 galaxy NGC3198 with a fitted curve which does not decrease with the distance
 237 but is instead constant. This is the discrepancy which is solved by postulating
 238 the existence of dark matter. After this the big question arises, what could this
 239 dark matter consist of? What is known so far lies in the name. It is called dark
 240 since there is no electromagnetic interaction and matter since it has gravitational
 241 interaction. This means that it can not be made up of any baryonic matter or
 242 anything in the Standard Model apart from neutrinos. The main interest of this
 243 thesis and also the main contributor to the rotational discrepancies is known as
 244 cold dark matter. This is due to the matter having a low speed, thus low kinetic
 245 energy, and have a high particle mass (In the GeV scale) [9, 12, 13]. This means
 246 however that neutrinos can not be a candidate, thus dark matter can not be made
 247 out of any standard model particles. There are several ideas to detected dark
 248 matter, [9]



(a) Rotation speed of planets in our solar system. Since the distance is quite small on an astronomical scale, there is no sign of dark matter. Based on data from [10].

(b) Rotation speed of matter in NGC3198 with a curve fitting and three different models, if only a dark model halo existed, if there was no dark matter and the correct, if both exist [11].

Figure 1.3: Different rotation curves, both for planets in our solar system and matter in the NGC3198 galaxy.

- Ordinary matter interacting with ordinary matter can produce dark matter, known as production. Which is the processes that occurs at particle accelerators.
- Dark matter interacting with ordinary matter can produce dark matter, known as direct detection.
- Dark matter interacting with dark matter can produce ordinary matter, known as indirect detection.

In this thesis the focus lies with production. There are several theories how to detect dark matter in proton-proton collisions such that occur at the LHC at CERN this is covered more in subsection 1.2.6.

1.2.5 Effective field theory

In quantum field theory the objective is usually to find the part of the Lagrangian which explains a type of interaction, known as the operator of the interaction and also to find the probability amplitude (cross-section) for a certain interaction. For complicated processes it is easier to employ certain conditions so that the small scale phenomena are simplified and the whole picture understood. This is known as using an effective field theory and the concept is explained in figure 1.4. The operator can be found through assuming the possible interactions and using the effective field theory [4]. The cross-sections can be found through the Feynman diagrams as described in subsection 1.2.1.

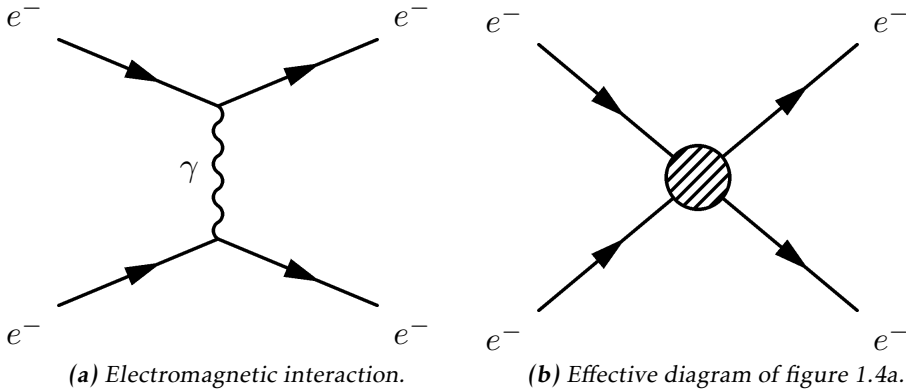


Figure 1.4: Feynman diagram of an electron-electron scattering, both as an ordinary diagram and as its effective theory version, where the details are hidden in the blob.

In this thesis the same effective field theory as in Refs. [12, 14] will be considered. The WIMP (usually denoted χ) is assumed to be the only particle in addition to the standard model fields. It is assumed that an even number of χ must be in every coupling. It is assumed that the mediator exists is heavier than the WIMPS, meaning that their interactions are in higher order terms of the effective field theory and thus not included in the operators. For simplicity, the WIMPS are assumed to be SM singlets, thus invariant under SM gauge transformations, and the coupling to the Higgs boson is neglected.

The operators used in this thesis are assumed to be quark bilinear operators on the form $\bar{q}\Gamma q$ where Γ is a 4×4 matrix of the complete set,

$$\Gamma = \{1, \gamma^5, \gamma^\mu, \gamma^\mu \gamma^5, \sigma^{\mu\nu}\} \quad (1.3)$$

This will dictate how the operators are written, more of why this is done can be found in [4, 12, 14].

This defines an effective field theory of the interaction of singlet WIMPs with hadronic matter. It is a non-renormalizable field theory which will break down when the mediator mass is close to the mass of the WIMP. The condition for this is derived in [14] and gives:

$$M > 2m_\chi \quad (1.4)$$

where m_χ is the mass of the WIMP and M is the mass of the mediator. There is also the requirement that:

$$M \lesssim 4\pi M_* \quad (1.5)$$

where M_* is the energy scale where the effective theory is no longer a good approximation.

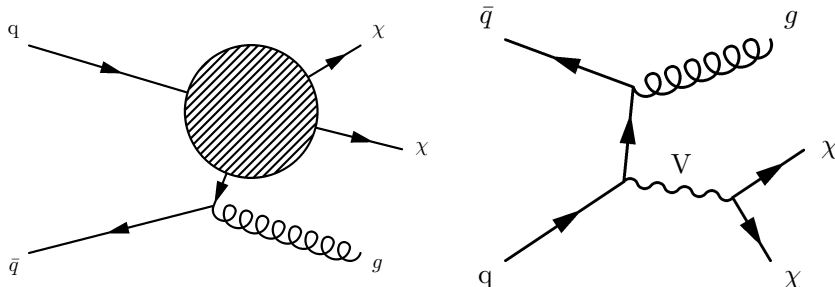
289 In this work, WIMPS are assumed to be Dirac fermions (half integer spin and is
 290 not its own antiparticle).

291 In table 1.1 the operators which are integrated out via the effective field theory
 292 and are of interest in this thesis are given.

Name	Initial state	Type	Operator
D1	qq	scalar	$\frac{m_q}{M_*^3} \bar{\chi} \chi \bar{q} q$
D5	qq	vector	$\frac{1}{M_*^2} \bar{\chi} \gamma^\mu \chi \bar{q} \gamma_\mu q$
D8	qq	axial-vector	$\frac{1}{M_*^2} \bar{\chi} \gamma^\mu \gamma^5 \chi \bar{q} \gamma_\mu \gamma^5 q$
D9	qq	tensor	$\frac{1}{M_*^2} \bar{\chi} \sigma^{\mu\nu} \chi \bar{q} \sigma_{\mu\nu} q$
D11	gg	scalar	$\frac{1}{4M_*^3} \bar{\chi} \chi \alpha_s (G_{\mu\nu}^a)^2$

Table 1.1: Table based on discussion in [13].

293 Where D denotes that the WIMPS are assumed to be Dirac fermions. These can all
 294 be described using figure 1.5a.



(a) Effective Feynman diagram explaining the D-operators. **(b)** Feynman diagram describing the vector mediator model.

Figure 1.5: Feynman diagrams describing the signal models used in this thesis.

295 Another model which is considered is a vector mediator model which is described
 296 by figure 1.5b.

1.2.6 Search for WIMPS

298 The search for WIMPS is based on a mono-jet analysis which is described in sub-
 299 section 1.3.6. This method revolves around a high energetic jet which arises from
 300 the gluon from figure 1.5b and momentum missing from the energy conservation.

301 This means that something has happened which the detectors can not detect. If
302 the models from subsection 1.2.5 can explain the missing energy, then a model
303 for WIMPS has been found.

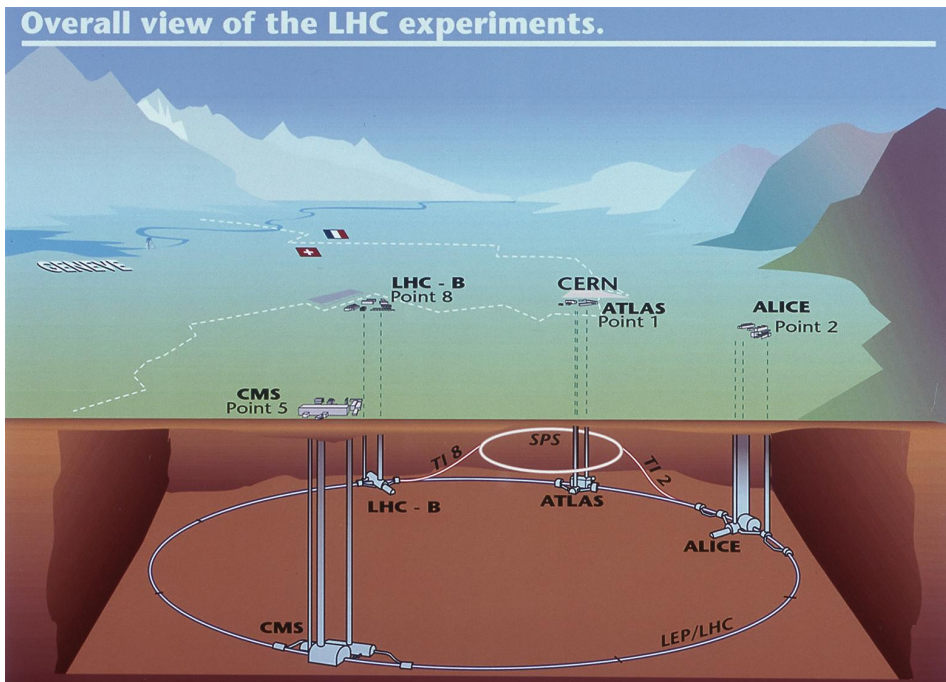
304 Since the search for WIMPS at the LHC is based on looking at the missing energy,
305 not actual detection, the experiment can not establish if a WIMP is stable on a
306 cosmological time scale and thus if it is a dark matter candidate [13]. This means
307 that if a candidate is found, it may still not be the dark matter that is needed to
308 explain the cosmological observations.

309 The different theories discussed in subsection 1.2.5 require some process in which
310 quarks and anti-quarks are produced. At ATLAS they have looked at proton-
311 proton collisions, in which they are produced, with 8 TeV center of mass energy
312 with out finding any excess of mono-jet events. This is why it is very interesting
313 that the LHC is undergoing a upgrade that will allow higher energy levels, see
314 subsection 1.3.7. With this the processes can be given higher energy and thus the
315 produced particles can be comprised of higher mass.

316 1.3 Experimental overview

317 1.3.1 LHC

318 The large hadron collider (LHC) is a particle accelerator located at CERN near
 319 Geneva in Switzerland, see figure 1.6. The accelerator was built to explore physics
 320 beyond the standard model and to make more accurate measurements of stan-
 321 dard model physics. Before it was shut down for an upgrade in 2012 it was able
 322 to accelerate two proton beams to such a velocity that each proton in them had
 323 an energy of 4 TeV which gives a center of mass energy, $\sqrt{s} = 8$ TeV. The proton
 324 beam is comprised of bunches of protons with enough spacing that bunch col-
 325 lisions can happen independent of each other. Apart from the energy, the rate at
 326 which the accelerator produces a certain process can be calculated through the
 327 instantaneous luminosity. For the LHC the instantaneous luminosity was 10^{34}
 328 $\text{cm}^{-2}\text{s}^{-1}$ [15] or $10\text{nb}^{-1}\text{s}^{-1}$ where 1 barn(b)= 10^{-24} cm^2 .



329 **Figure 1.6:** Figure showing the LHC and the different detector sites[16].

330 The instantaneous luminosity, often just denoted luminosity, can be defined in
 331 different ways depending on how the collision takes place. For two collinear
 intersecting particle beams it is defined as:

$$\mathcal{L} = \frac{f k N_1 N_2}{4\pi \sigma_x \sigma_y} \quad (1.6)$$

332 where N_i are the number of protons in each of the bunches, f is the frequency
 333 at which the bunches collide , k the number of colliding bunches in each beam,
 334 and σ_x (σ_y) is the horizontal (vertical) beam size at the interaction point. Since
 335 the instantaneous luminosity increases quadratically with more protons in each
 336 bunch, increasing the number of protons would be a good strategy to increase
 337 the instantaneous luminosity. However aside from the difficulties to create and
 338 maintain a beam with more particles, a large N_i increases the probability for
 339 multiple collisions per bunch crossing, referred to as pile-up. Pile up will be a
 340 key aspect which is described more in subsection 1.3.5.

341 The expected number of events can be calculated by using the instantaneous lu-
 342 minosity through the following:

$$N = \sigma \int \mathcal{L} dt \equiv \sigma \mathcal{L} \quad (1.7)$$

343 where \mathcal{L} is the integrated luminosity and σ is the cross section which is often
 344 measured in barn. The integrated luminosity is a measurement of total number
 345 of interactions that have occurred over time. Before the LHC was shut down \mathcal{L}
 346 was 20.8 fb^{-1} .

347 The cross section, as explained in subsection 1.2.1, is a measure of the effective
 348 surface area seen by the impinging particles, and as such is expressed in units
 349 of area. The cross section is proportional to the probability that an interaction
 350 will occur. It also provides a measure of the strength of the interaction between
 351 the scattered particle and the scattering center. Further details can be found in
 352 reference [17].

353 1.3.2 ATLAS

354 As seen in figure 1.6, there are several detectors at the LHC. One of these is
 355 ATLAS which is a general purpose detector that uses a toroid magnet. Its goal
 356 is to observe several different production and decay channels. The detector is
 357 composed of three concentric sub-detectors, the Inner detector, the Calorimeters
 358 and the Muon spectrometer [18].

359 The Inner detectors main task is to detect the tracks of the particles. It also mea-
 360 sures the position of the initial proton-proton collision.

361 The Calorimeters, electromagnetic and hadronic, are used to calculate the energy
 362 contained in the different particles. The electromagnetic detects particles which
 363 are charged, and the hadronic those which are neutral.

364 The Muon spectrometer is used to detect signs of muons, which will simply pass
 365 through the other detectors without leaving a trace. It also calculates the energy
 366 and momentum of the muons.

367 The neutrinos escape the ATLAS experiment without being detected, and in this
 368 thesis it is assumed that WIMPS pass through all the detectors without leaving
 369 any trace.

370 1.3.3 Coordinate system

371 The coordinate system of ATLAS, seen in figure 1.7 is a right-handed coordinate
 372 system with the x-axis pointing towards the centre of the LHC ring, and the z-axis
 373 along the tunnel/beam (counter clockwise) seen from above. The y-axis points up-
 374 ward. The origin is defined as the geometric center of the detector. A cylindrical
 375 coordinate system is also used for the transversal plane, (R, ϕ, Z) . For simplicity
 376 the pseudorapidity of particles from the primary vertex is defined as:

$$\eta = -\ln(\tan \frac{\theta}{2}) \quad (1.8)$$

377 where θ is the polar angle (xz-plane) of the particle direction measured from
 378 the positive z-axis. η is through this definition invariant under boosts in the z-
 379 direction.

380 It is quite common to calculate the distance between particles and jets in the
 381 (η, ϕ) space, $d = \sqrt{(\Delta\eta)^2 - (\Delta\phi)^2}$.

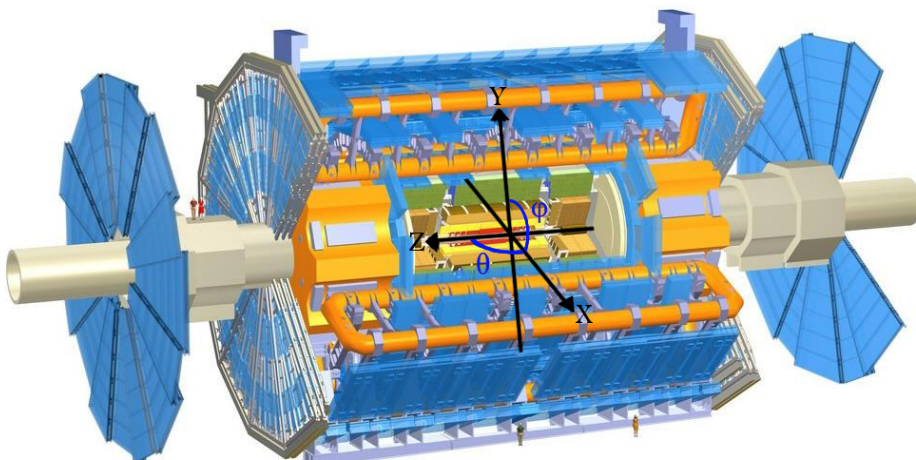


Figure 1.7: The ATLAS detector and the definition of the orthogonal Cartesian coordinate system. Image altered from[19]

382 1.3.4 Reconstructing data

383 To be able to compare the simulated data to real data it is important to include
 384 effects of the detectors. This is done using so called smearing functions which try
 385 to emulate the reconstruction of data.

386 The reconstruction process of data [18] is based on what response is given from
 387 the detectors. It is affected by pile-up and the energy of that which is detected.
 388 This process is not specifically used in the thesis, however the smearing functions
 389 are discussed in section 2.1.

390 **1.3.5 Pile-up**

391 Pile-up is the phenomena that several proton-proton collisions occur simultaneously.
 392 The number of pile-up is defined as the average number of proton-proton
 393 collisions that occur per bunch crossing per second. It is denoted as $\langle \mu \rangle$. μ can
 394 be calculated by adjusting a Poisson distribution to fit the curve created by the
 395 number of interactions per bunch crossing at a given luminosity. When this is
 396 done μ will be the mean value of the Poisson distribution.

397 **1.3.6 Mono-jet analysis**

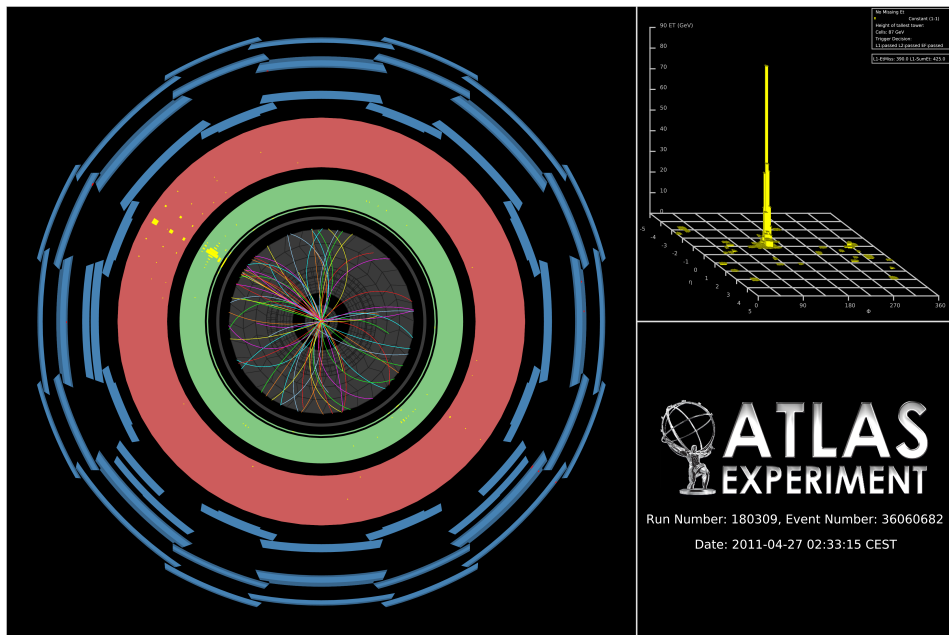


Figure 1.8: Image of an actual mono-jet event recorded by the ATLAS experiment [20].

398 When measuring the transversal energy one can in some interactions find incon-
 399 sistencies, such as jets that are in excess in one direction. In figure 1.8 one can see
 400 a high energetic jet which gives an excess of transversal energy in one direction
 401 after the collision. Since there is no balancing jet there must be transverse energy
 402 that is not detected, denoted E_T^{Miss} , since it was close to zero before the collision.
 403 This gives an indication that there energy to balance this that simply can not be
 404 detected. This could for instance be neutrinos or the sign of a new particle.

405 E_T^{Miss} is the modulus of the E_T^{Miss} vector which is defined as:

$$E_T^{\vec{Miss}} = - \sum \vec{jet}_T - \sum \vec{e}_T - \sum \vec{\mu}_T - \sum \vec{\tau}_T - \sum \vec{\gamma}_T \quad (1.9)$$

406 Jets are hadrons which travel in the same direction and are usually created from

407 hadronization of a quark or a gluon in a collision. Usually jets are composed of a
 408 lot of energetic hadrons.

409 Since the jets are created from quarks or gluons, measuring a jet results in more
 410 information about the collision.

411 There are two main classes of events, signal and background. The signal corre-
 412 sponds to events that would arise from one of the processes in subsection 1.2.5.
 413 However to know that the missing energy is sign of the signal then one must un-
 414 derstand all the other components that could contribute to the missing energy.
 415 Also there must be an excess of missing energy from what is expected from the
 416 background.

417 The background comprises of standard model processes that can mimic the mono-
 418 jet signature.

419 1.3.7 Phase II high luminosity upgrade

420 At the moment, the whole LHC is undergoing a step by step upgrade program
 421 which will be finalized around 2022-2023, denoted the high luminosity upgrade, or
 422 HL-upgrade. The upgrade consists of different stages, meaning that the upgrade
 will halt for periods so that experiments can take place. In figure 1.9 one can see

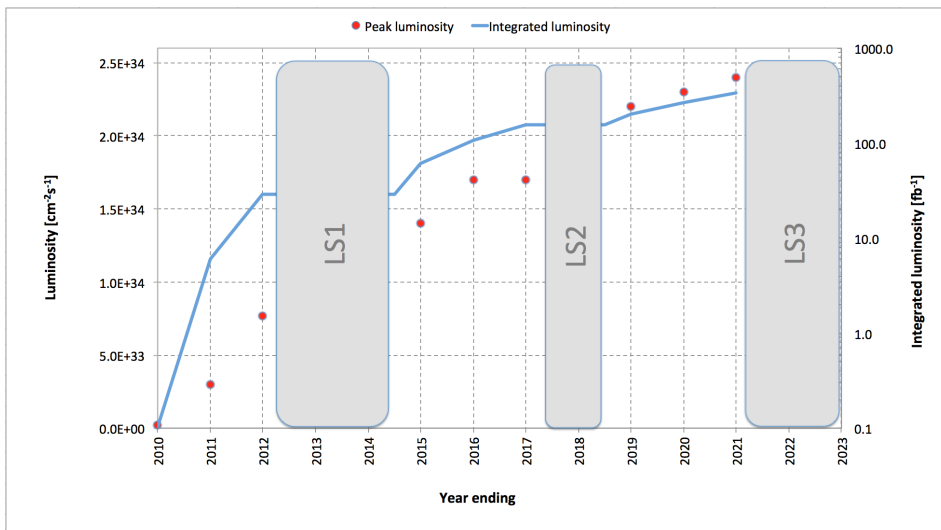


Figure 1.9: A graph showing the upgrading timetable with the instantaneous luminosity, denoted luminosity, and integrated luminosity expected in the different stages.

423
 424 the three proposed upgrades. The period before LS1 is denoted phase 0, after
 425 LS1 and before LS2 phase I and after LS3 phase II.

426 LS1 is the upgrade which will take the LHC to its designed performance.

- 427 LS2 will take the LHC to the ultimate designed instantaneous luminosity.
 428 LS3 which is the focus of this thesis, will increase the instantaneous luminosity
 429 even more. Though for this to happen a modification of the whole LHC
 430 must be done, instead of just an upgrade and maintenance as before.

431 The following is expected for the experiments done after phase II:

Entity	Expected	Last run (2012)
Instantaneous luminosity	$\mathcal{L} \sim 50 \text{ nb}^{-1} \text{s}^{-1}$	$\mathcal{L} \sim 10 \text{ nb}^{-1} \text{s}^{-1}$
Integrated luminosity	$\mathcal{L} = 1000 - 3000 \text{ fb}^{-1}$	$\mathcal{L} = 20 \text{ fb}^{-1}$
Pile-up	$\langle \mu \rangle = 140$	$\langle \mu \rangle = 20$
Center of mass energy	$\sqrt{s} = 14 \text{ TeV}$	$\sqrt{s} = 8 \text{ TeV}$

Table 1.2: Expected running values for the Phase II HL-upgraded LHC with older values for comparison [21].

- 432 Where it should be noted that the integrated luminosity indicates the total amount
 433 of data which will be collected after the upgrade is completed before the next up-
 434 grade takes place.

435 1.3.8 Monte Carlo simulation

- 436 As mentioned before, in this thesis only emulated data has been used. This data
 437 is created by using a Monte Carlo simulation of the background processes and
 438 the expected signal. To do this a program called MadGraph is used.
 439 MadGraph [22] starts with Feynman diagrams and then generates simulated events
 440 based on lots of different parameters.
 441 PYTHIA [23] is a package which adds the correct description of jets to MadGraph
 442 by including hadronization. The correct description of pile-up comes from other
 443 ATLAS software.
 444 The tool to access all this data and analyse it a tool called ROOT, which is used
 445 for programming high energy physics related tools [24].

2

Validation of smearing functions

448 One might assume that using a Monte Carlo simulation it would be easy to model
449 and emulate the whole process, from collision to detection and reconstruction in
450 the upgraded LHC. It is possible, but it requires a lot of computing power. Instead
451 one can use one simulation and a mathematical model to calculate the estimated
452 response in the detector. This was validated and used in this thesis to be able to
453 create the data needed for further analysis.

454 This was done by using a Monte Carlo simulation of a proton-proton collision and
455 applying the official Truth to reco code, also known as the smearing functions,
456 that was developed using previous studies [1, 25]. to simulate how the detector
457 and the reconstruction is affected by the increased luminosity and the pile-up
458 that comes with this.

459 The code uses the experimental data from the previous studies to smear the re-
460 constructed energy and momenta, it is from this that the name smearing func-
461 tions comes. The key feature of those studies were that the direction of the mo-
462 mента is unaffected and that only jets and E_T^{Miss} are affected by pile-up. This was
463 confirmed in previous studies and were thus not incorporated into the smearing
464 functions, more in section 2.1.

465 2.1 Smearing functions

466 **Put in introduction? The particles that are directly detectable in ATLAS are:**
467 electron, photon, muon, tau. Aside from this jets can be detected, and from this
468 E_T^{Miss} can be calculated.

469 This means that the all detectable entities must have their own smearing func-
470 tions.

471 E_T^{Miss} , the missing transversal energy, which was discussed in subsection 1.3.6, is
472 calculated by knowing that there should be energy conservation in the collision.
473 It is comprised of different parts, one from neutrinos, one from errors in the
474 other measurements and one from (hopefully) new physics.

475 The jet and E_T^{Miss} are the only "parts" which are not unique particles instead they
476 are based either on a shower of particles or the energy which is missing from
477 the conservation of transversal energy. Thus, the pile-up dependence here must
478 simply come from the fact that it is hard to separate the different jets and that
479 with several different collisions occurring makes it hard to accurately measure
480 the total energy.

481 The electron and photon have the same smearing since they are both detected
482 in a similar way. Perhaps add more to the introduction about each part of the
483 detector. or simply write that here?

484 The muon is special since it is detected in the muon spectrometer.

485 Tau is detected similarly to electron and photon.

486 These smearing functions are designed so that they take into account the effi-
487 ciency of the different detectors, limitations as well as their dependence on pile-
488 up. They also take into account how all this varies depending on the measured
489 entries energy or momenta.

490 The terminology is that data before smearing, simulated data, is denoted as data
491 at a truth level or truth data. Data after smearing, which is comparable to what
492 is measured, reconstructed or reco data as discussed in subsection 1.3.4.

2.2 Validation

493 To validate the smearing functions a comparison with [25] was made where the
 495 standard deviation, depending on the energy or momentum value of an entity,
 496 was given, see section 2.4. To calculate this some simulated processes were needed
 to extract data, see table 2.1.

Data	Process
Electron	$W \rightarrow e\nu$
Muon	$W \rightarrow \mu\nu$
Tau	$W \rightarrow \tau\nu$
γ	$\gamma + \text{Jet sample}$
Jets	Jet sample
E_T^{Miss}	$Z \rightarrow \nu\nu + \text{Jet sample}$

Table 2.1: Different processes from where data has been taken. Each sample is a simulation of a physical process, the simulation names can be found in appendix A

497
 498 By plotting the data for each data point before and after the smearing function,
 499 for that data point had been used, one can verify the functions. This is done
 500 looking at the reco data for a given truth energy or momentum value. Since the
 501 smearing functions take a lot of things into account the match will not be a fine
 502 line, see figure 2.3b.

503 By fitting a Gaussian curve to this data will then result in the mean value, and
 504 the standard deviation. The mean value is not of interest for the purposes of
 505 the thesis, though the standard deviation is since it is this which is used in the
 506 validation. The standard deviation is equivalent to RMS (Root mean square) and
 507 is also known as the resolution of the data. It will from here on be denoted RMS
 508 or σ .

509 This resolution is then compared to previous results, [25], and finally confirmed
 510 or demented.

511 To get enough and thorough statistics enough data must be available for a given
 512 truth energy or momenta and the analysis must be specific enough to only look
 513 at a minute interval around this point.

514 2.3 Results

515 As discussed above, the method was to plot the data against its smeared counter-
516 part and through this determine the RMS, (σ) to see if it conforms to the expected
517 values.

518 Since there are only slightly differences depending on pile-up these are not shown
519 except for E_T^{Miss} and jets. Also only one energy value is shown for simplicity,
520 though the comparison was done for different energy values.

521 Pile-up is fixed at 60 is nothing else is said used simply as a benchmark.

522 The images are, as the comparison, often divided depending on the different η
523 values.

524 All results are summarized in table 2.5.

2.3.1 Electron and photon

Since these interact very similarly in the detector, their smearing functions are identical. The slice value represents at which value of unsmeared energy or momentum this smearing occurs.

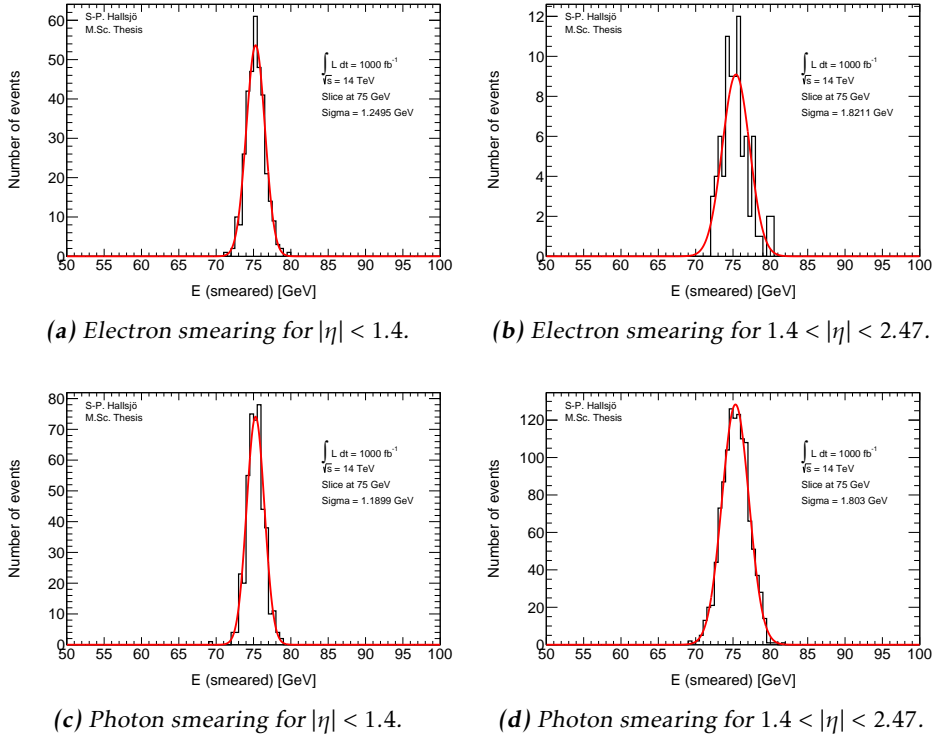


Figure 2.1: Photon and electron smearing plots.

529 **2.3.2 Muon**

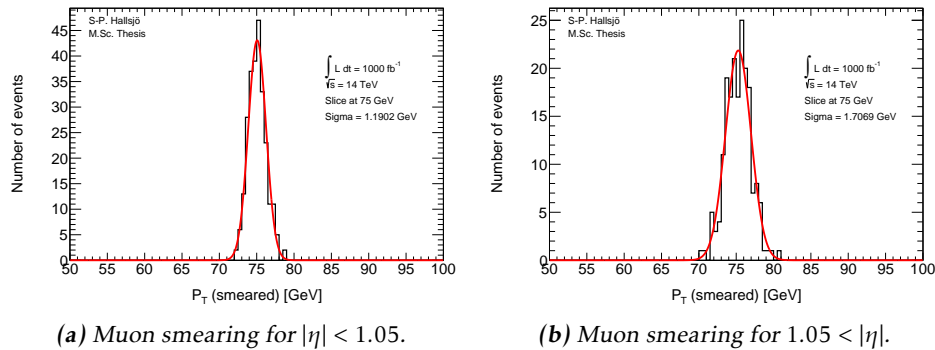


Figure 2.2: Muon smearing plots.

530 **2.3.3 Tau**

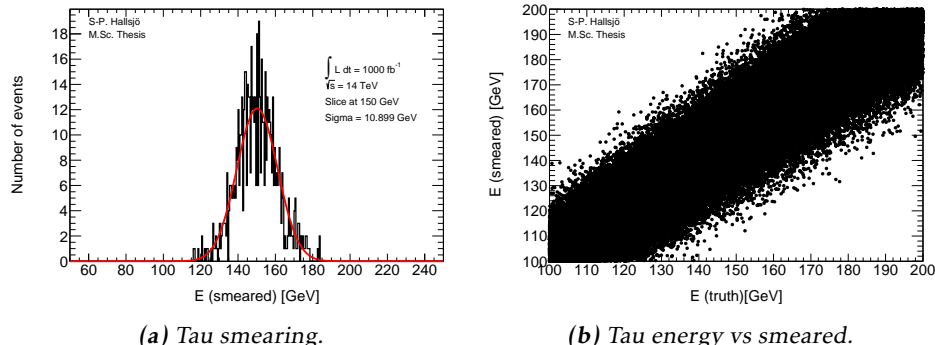


Figure 2.3: Tau smearing and energy vs smearing plot.

2.3.4 Jets

Jets as described in subsection 1.3.6, are hadronic showers. The smearing functions are divided into four different regions depending on the angle η .

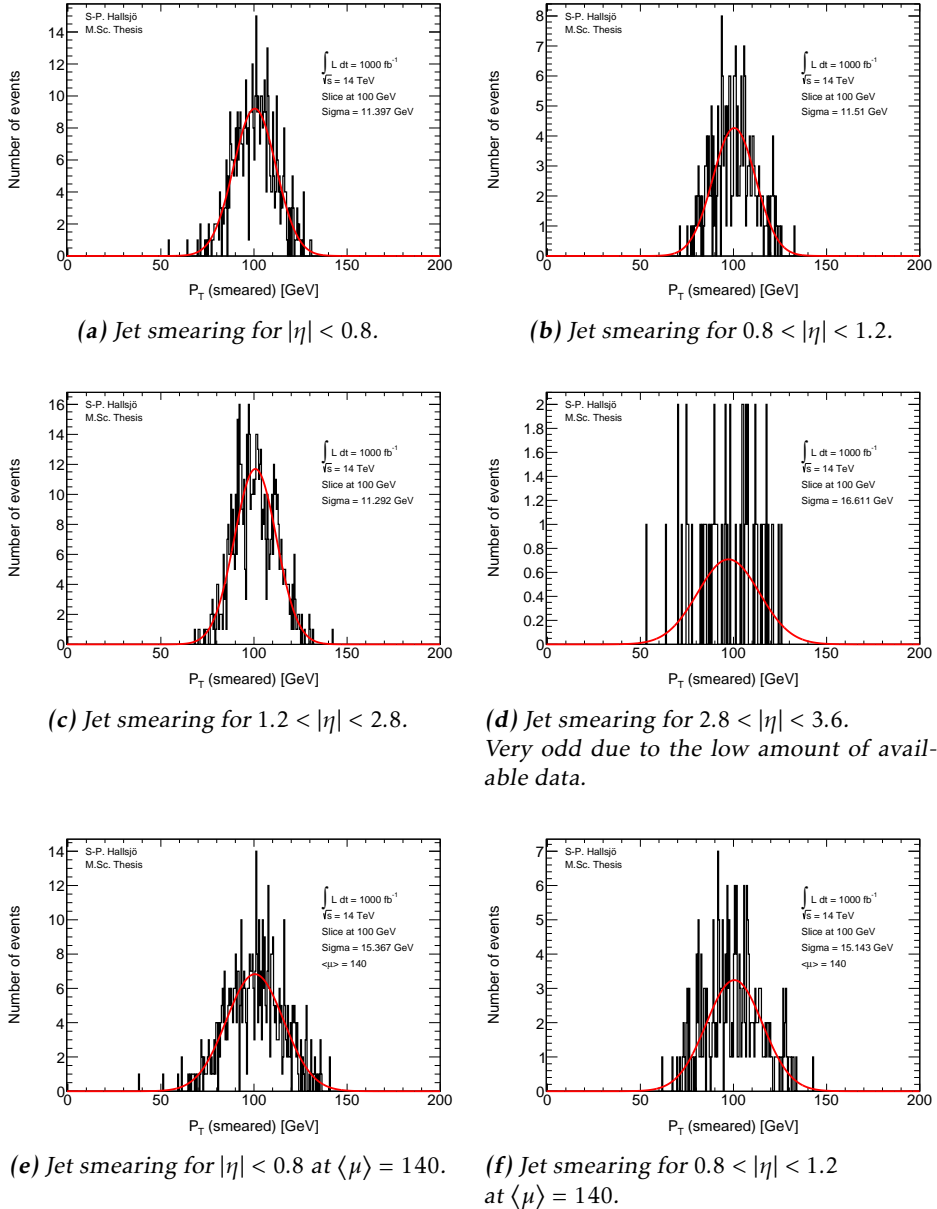


Figure 2.4: Jet smearing plots.

534 2.3.5 Missing Transversal Energy

535 These figures are given as smeared value from origin, thus at 0 it represents that
 536 the energy is unsmeared, compared to the others where the slice value represents
 537 the unsmeared.

538 Here the E_T^{Miss} is projected down to the x- and y-axis, since these are the transver-
 539 sal axes, to be smeared.

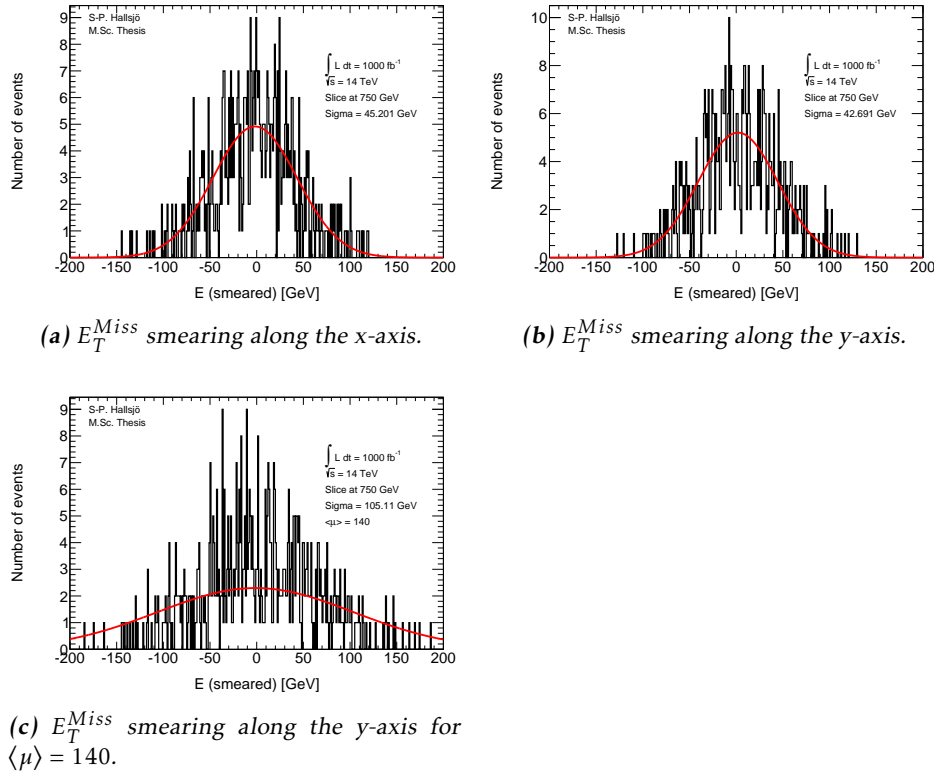


Figure 2.5: E_T^{Miss} smearing plots

540 2.4 Expected results

541 The expected response has been calculated and taken from [25].

542 The independence of pile-up for leptons and photons is backed up in previous
543 research, for instance [1, 26] were the first states:

544 “The uncertainty due to pile-up was investigated by comparing
545 simulated MC samples with and without pile-up and was found to be
546 negligible”

547 This is also confirmed in other internal documents.

548 To validate the smearing code comparisons were made with [25] which gave the
549 following formulation for the expected RMS:

Process	Absolute RMS
Electron & photon	$\sigma = 0.3 \oplus 0.1\sqrt{E(GeV)} \oplus 0.01E(GeV), \eta < 1.4$ $\sigma = 0.3 \oplus 0.15\sqrt{E(GeV)} \oplus 0.015E(GeV), 1.4 < \eta < 2.47$
Muon	$\sigma = \frac{\sigma_{id}\sigma_{ms}}{\sigma_{id} \oplus \sigma_{ms}}$ $\sigma_{id} = P_T(a_1 \oplus a_2 P_T)$ $\sigma_{ms} = P_T(\frac{b_0}{P_T} \oplus b_1 \oplus b_2 P_T)$
Tau	$\sigma = (0.03 \oplus \frac{0.76}{\sqrt{E(GeV)}})E(GeV)$
Jet	$\sigma = P_T(GeV)(\frac{N}{P_T} \oplus \frac{S}{\sqrt{P_T}} \oplus C)$
E_T^{Miss}	$\sigma = (0.4 + 0.09\sqrt{\mu})\sqrt{\sum E(GeV) + 20\mu}$

Table 2.2: Expected absolute RMS.

550 • For muon: All parameters are given in table 2.3.

551 • For tau: Fixed at 3 prong. 1 prong exists though was not used in this thesis.
552 Where prong refers to the different amount of tracks that from which they
553 were reconstructed.

554 • For jet: All parameters are given in table 2.4 where $N = a(\eta) + b(\eta)\mu$.

	a_1	a_2	b_0	b_1	b_2
$ \eta < 1.05$	0.01607	0.000307	0.24	0.02676	0.00012
$ \eta < 1.05$	0.03000	0.000307	0.00	0.03880	0.00016

Table 2.3: Parameters used in the muon smearing function take from [25].

$ \eta $	a	b	s	C
0-0.8	3.2	0.07	0.74	0.05
0.8-1.2	3.0	0.07	0.81	0.05
1.2-2.8	3.3	0.08	0.54	0.05
2.8-3.6	2.8	0.11	0.83	0.05

Table 2.4: Parameters used in the jet smearing function taken from [25].

Process	RMS [GeV]	Error in RMS	Expected RMS	Significance
Electron low η	1.24948	0.0481987	1.18427	1.35286
High η	1.8211	0.141329	1.74446	0.542334
Photon low η	1.18986	0.0400187	1.18427	0.139734
High η	1.80297	0.0374312	1.74446	1.56323
Muon low η	1.19016	0.0524938	1.49789	5.86235
High η	1.70694	0.0882606	2.18318	5.39575
Tau	10.8992	0.299761	10.3388	1.86975
Jet low η	11.3974	0.351391	11.5983	0.571586
$\langle \mu \rangle = 140$	15.3673	0.473783	15.7721	0.854499
Mid low η	11.5096	0.518872	11.9352	0.820407
$\langle \mu \rangle = 140$	15.1427	0.682649	15.9515	1.18475
Mid high η	11.2916	0.310314	10.9439	1.12021
High η	16.6112	1.52891	13.5	2.03491
E_T^{Miss} x-axis	45.2013	1.35426	48.4483	2.39762
E_T^{Miss} y-axis	42.6906	2.27904	48.4483	4.50154
$\langle \mu \rangle = 140$	105.109	12.239	87.2812	1.45667

Table 2.5: RMS values.

- 555 • Where the given RMS is still the absolute.
 556 • The significance is the standard deviation of between the expected and cal-
 557 culated with respect to the error.

558 2.5 Discussion

559 2.5.1 Smearing independent on pile-up

560 From the validation done it was interesting to note that the smearing functions
561 were created from previous studies, [1, 26], which had shown that leptons and
562 photons are not affected by pile-up. This may seem incredible however it be-
563 comes quite logical when one understands how the detectors work. To be able to
564 detect particles the detectors must detect an excess of energy which comes from
565 a particle passing through. This should not be distorted by an increased pile-up.
566 The amount of particles passing through will of course increase, but the detec-
567 tions should be unaffected as well as the recreation of the events. However with
568 the same logic it makes sense that jets and E_T^{Miss} are quite affected since they
569 are combined of several parts, either hadronic particles or by all the transversal
570 missing energy.

571 Another interesting part is how the effect diminishes with and increasing energy.
572 As seen above, and through the the formula, for the high energies which were of
573 interest here the effect is minimal.

574 2.5.2 Comparison to expected results

575 One of the major problems in the comparison was to get the significance of the
576 Gaussian fit to be calculated correctly. The tool ROOT has a lot of different fea-
577 tures which made this task somewhat difficult. Also since this is a statistical
578 property there is a statistical fluctuation in the result.

579 Another was to retrieve the correct values from the paper, [25], since it was un-
580 clear if the values given were absolute or scale dependent. This has now been
581 corrected in a new version of the paper.

2.6 Conclusion

582 The smearing functions work as intended within 5.8 sigma, however when using
584 a test box and averaging the sigmas one ends up with half of this for the extreme
585 cases, muons and E_T^{Miss} y-axis.

3

Evaluating dark matter signals

588 The main goal of the thesis is to investigate if certain dark matter signals can
589 be detected after the high luminosity upgrade. One immediate worry is that the
590 background will be large in comparison to the signal, making the signal undetectable.
591

592 The following signals models have been used: The signal models are given in
593 appendix A along with the background. The different models were discussed in
594 part in subsection 1.2.5 and some more in this chapter.

595 Each of these has been evaluated in different signal regions and the detectability
596 has been evaluated using a statistical P-value. This process has been performed
597 at different pile-up values.

598 **What background existed? How was it simulated in MC? Should that be here
599 or in appendix?**

600 Dont mention, but good to know. Used METpt in all histograms, with the weight
601 as in main.C and mainclass.C.

602 3.1 Signal to background ratio

603 What I am doing now, looking at what signal? What are the different background
604 processes? What and why was the weight used?

605 Signals should be explained somewhat in the introduction.

606 Look at presentation, is it worth bringing up the first signal regions when the
607 data has already been filtered? Should that be here?

608 3.1.1 Selection criteria

609 What criteria were used and more importantly why? It is quite important that
 610 you can explain why this was used.

611 For different purposes different selection criteria or regions are used. These are a
 612 set of criteria specified to enhance the area of interest. For instance, if simulating
 613 a specific signal one wants to find as many ways as possible to diminish the back-
 614 ground. This so that when searching experimentally, the signal will be easier to
 615 detect.

616 These can be quite general cuts, there are only some things to take into consider-
 617 ation.

- 618 • If experimental, what limitations are set by the detectors? Are there some
 619 criteria already?
- 620 • If simulated, is there some criteria set in the generator?
- 621 • Are there criteria which must be set since there is to much uncertainty in
 622 the data? or a large effect of pile up?

623 3.1.2 Verifying background data

624 To verify that the background data was correct it was compared with [27], in
 625 which the luminosity if 10 fb^{-1} and thus the expected values from the paper
 626 scaled up with a factor 100. **Also, somewhat unexpectedly is that the differ-
 627 ence in center of mass energy required the cross-sections to be much lowered
 628 than compared with the upgrade.** The signal region used in the article were the
 following:

Selection Criteria		
Jet veto, require no more than 2 jets with $p_T > 30 \text{ GeV}$ and $ \eta < 4.5$		
Lepton veto, no electron or muon		
Leading jet with $ \eta < 2.0$ and $\Delta\phi(\text{jet}, E_T^{\text{Miss}}) > 0.5$ (second-leading jet)		
signal region	SR3p	SR4p
minimum leading jet p_T (GeV)	350	500
minimum E_T^{Miss} (GeV)	350	500

629 *Table 3.1: The signal regions*

630 The article has several different signal regions, the difference is the last item, un-
 631 fortunately since the simulated events are already filtered before the analysis only
 632 one of the regions could be used.

633 NEW WITH 350 as SR3 and 500 as SR4 and expected (Scaled to 1000 fb^{-1}) thus
 634 scaled a factor 100 since luminosity is only a measurement of the amount of data
 635 and does not change anything physical.

Process	SR3p	Expected SR3p	SR4p	Expected SR4p
$Z \rightarrow \nu\nu$	140298	152000	25250.3	27000
$W \rightarrow \tau\nu$	40700.8	37000	5861.74	3900
$W \rightarrow e\nu$	11229	11200	1506.58	1600
$W \rightarrow \mu\nu$	13727.1	15800	1872.32	4200
Total background	205955	218000	34491	36700

Table 3.2: Comparison of the simulated and expected events from [27].

636 In table 3.2 a comparison has been made. It can be seen that the simulated events
 637 and expected events coincide on all accounts apart from $W \rightarrow \tau\nu$, $W \rightarrow \mu\nu$ and
 638 thus the total as well. **This can be explained by better separation of μ, τ and**
 639 **missing energy.** Tau can not be reconstructed as jets in the code, they can in
 640 reality!

641 3.1.3 Figures of merit

642 **P-value, info from Majas phd thesis. Is there a source? Should there be a fig-**
 643 **ure?**

644 To be able to evaluate different signal regions and different signal models, a figure
 645 of merit p is used. The value p is the probability for an assumed hypothesis
 646 to be correct, thus a good signal region will yield a low value. The assumed
 647 hypothesis is that the background and its fluctuations is measured over the signal
 648 plus background.

649 Assuming the expected number of background events are $B \pm \sigma_B$ where σ_B is the
 650 quadratic sum of the statistical error from Monte Carlo, the statistical error from
 651 the control region and the systematic errors. The expected number of signals is S ,
 652 assumed without fluctuation.

653 If no uncertainty in B or S is assumed, then the number of expected events, N , in
 654 the signal region should follow a Poisson distribution as such:

$$P(N|S+B) = \frac{e^{-(S+B)}(S+B)^N}{N!} \quad (3.1)$$

655 However since there is an uncertainty in the background, the probability distri-
 656 bution $P(N|S+B)$ must be convoluted with a Gaussian function:

$$G(N_B|B, \sigma_B) = \frac{1}{\sigma_B \sqrt{2\pi}} e^{-\frac{(N_B - B)^2}{2\sigma_B^2}} \quad (3.2)$$

where N_B is the expected number of background events. The convolution is done

using N_B as N resulting in the total probability density function:

$$\begin{aligned} F(N|S+B, \sigma_B) &= P(N|S+N_B)*G(N_B|B, \sigma_B) = \\ &= \int_{-\infty}^{\infty} P(N|N_B - (S + B))G(N_B|B, \sigma_B)dN_B \end{aligned} \quad (3.3)$$

657 This leads to the probability of the signal plus background fluctuation to B events
 658 being obtained by summing the probability function from $N=0$ to $N=B$.

$$p = \sum_{i=0}^B \int_{-\infty}^{\infty} P(i|N_B-(S+B))G(N_B|B, \sigma_B)dN_B \quad (3.4)$$

659 3.1.4 D5 operators

660 Discuss M^* , and the difference in mDM. From presentation given, 3-4 April.
 661 Was discussed in part in subsection 1.2.5
 662 As described in the introduction **reference?**, one of the signals is modelled using
 663 the D5 operator. In this thesis two different scenarios were used, one at a dark
 664 matter mass of 50 GeV and one at 400 GeV.

665 3.1.5 Light vector mediator models

666 Discuss M_m , width, and the difference in mDM. From presentation given, 3-4
 667 April.
 668 Was discussed in part in subsection 1.2.5
 669 As described in the introduction **reference?**, the other signal model is a vector
 670 mediator model. The data available is: two different widths $M/3$ and $M/8\pi$.
 671 **M?!**? two different mDM, 50 GeV and 400 GeV and finally a variety of mediator
 672 masses.

673 3.1.6 Susy models?

674 3.2 Other selection criteria and observables

675 New signal regions.

676 3.3 Mitigating the effect of the high luminosity

677 Something pile-up Something as seen in validation of... the effect is quite minute
 678 for high energy values and does not at all affect leptons or photons. Mention that
 679 the effect is on a trigger level, that the lowest SR will be lost.

680 Even though this was envisioned as the primary focus of the thesis, it was shown
 681 that the effect of pile-up is minute for these high signal regions. Thus the focus

Selection Criteria

Jet veto, require no more than 2 jets with $p_T > 30\text{GeV}$ and $|\eta| < 4.5$

Lepton veto, no electron or muon

Leading jet with $|\eta| < 2.0$ and $\Delta\phi(\text{jet}, E_T^{\text{Miss}}) > 0.5$ (second-leading jet)

signal region	SR0	SR1	SR2	SR3	SR4
minimum leading jet p_T (GeV)	120	350	600	800	1000
minimum E_T^{Miss} (GeV)	120	350	600	800	1000
signal region	SR0	SRa	SRb	SRc	SRd
minimum leading jet p_T (GeV)	350	350	350	350	350
minimum E_T^{Miss} (GeV)	120	350	600	800	1000

Table 3.3: The new signal regions

682 was shifted to perform a more in-depth mono-jet analysis of different DM signal
683 models.

684 3.4 Results

685 3.4.1 Limit on M^*

686 The mass suppression scale. Give at 1000fb^{-1} . And for the different signal re-
687 gions. **ASK CHRISTOPHE FOR A GOOD EXPLANATION OF M^* and why**
688 **there can be limits!**

689 For the new signal regions: **Include a table of the limits for truth and Reco.**

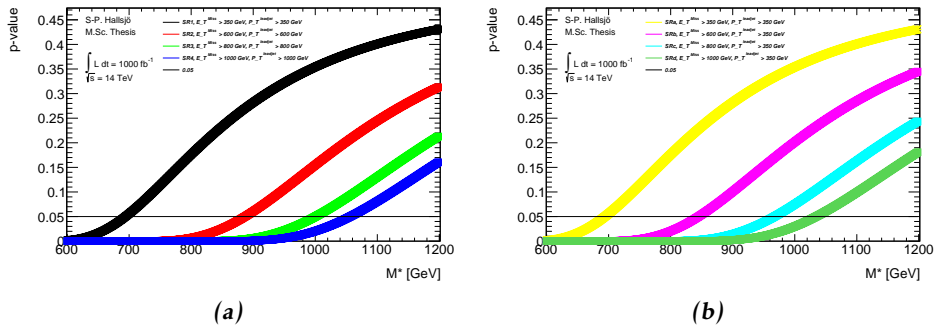


Figure 3.1: On a truth level.

690 3.4.2 Effect of pile-up on M^*

691 Hardly any effect. 10 % or in that vicinity.

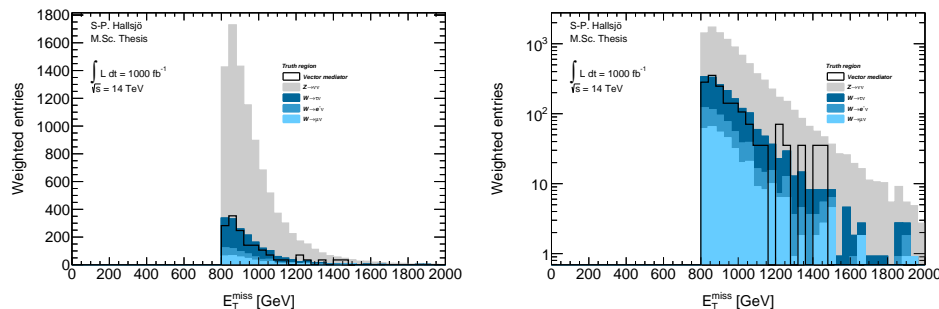
692 3.4.3 Previous results

693 Valerios paper for instance. Preliminary note that much better results for 1000fb-1
 694 and 14TeV.

695 The whole discussion with Steven and David.

696 3.4.4 Limit on mediator mass

697 Are there previous results? Signal vs background plot in normal and log scale for
 698 one of the vector mediator models, to be able to evaluate all the different models
 699 the so called p-value was used in different signal regions. Below are two figures
 700 showing one of the vector mediator models in SR3.



(a) Signal on background plot for E_T^{Miss} on reco level in SR3. (b) The same as a) with log scale on the y-axis

Figure 3.2: Signal on background plot to illustrate the a general plot.

701 To set a limit on the mediator mass the p-value was calculated in different sig-
 702 nals regions for the different signal models with different mediator mass. This
 703 resulted in the following plot:

704 3.4.5 Effect of pile-up on mediator mass

705 Check the different cases for reco and truth to see what happens.

706 3.5 Discussion

707 3.6 Conclusion

4

Results and Conclusions

710 **4.1 Validation of smearing functions**

711 Have some discussion.

712 Result they appear to work as expected, the reference paper was a bit unclear, I
713 leave my writing as a better reference.

714 **4.2 Signal to background ratio**

715 **4.2.1 Limit on M^***

716 **4.2.2 Limit on mediator mass**

717 **4.3 Other selection criteria and observables**

718 **4.3.1 Limit on M^***

719 **4.3.2 Limit on mediator mass**

720 **4.4 Mitigating the effect of the high luminosity**

721 **4.5 Recommendations to mitigate the effect of the
722 high luminosity**

723 Keep to a higher energy region, or signal region.

724 4.6 Suggestions for future research

725 With more time, search for new signal regions, the only solution now for the HL
726 is to go up in energy. Since none of the other parameters (eta,phi etc) seem to be
727 altered these can not be used. Is there something that has been overlooked?

728 Test the effect of pile-up for lower signal regions? See if the effect is as great as
729 predicted.

730 Explore other theoretical models for dark matter, other d operators etc. Models
731 that are based on Supersymmetry and not just effective theories.

732 Sätt av ett kort kapitel sist i rapporten till att avrunda och föreslå räkningar för
733 framtida utveckling av arbetet.

734 Saving as reference. test citing as: Here we cite Duck [28] [28].

735 If the above works, remember to edit myreferences.

Appendix

737

A

738

Datasets

739 A.1 Background processes

740 A.1.1 Validation

741 For the validation the following datasets were used, with a filter at generator level
742 at 450GeV for lead jet and MET.

743 mc12.157539.sherpa_ct10_znunupt280d4pd.v03 mc12.157534.sherpa_ct10_wenupt200d4pd.v03

745 mc12.157535.sherpa_ct10_wmunupt200d4pd.v03

746 mc12.157536.sherpa_ct10_wtaunupt200d4pd.v03

747 mc12.129160.pythia8_au2cteq6l1_perf_jf17d4pd.v03

748 mc12.129160.pythia8_au2cteq6l1_perf_jf17d4pd.v04

749 mc12.129170.pythia8_au2cteq6l1_gammajet_dp17d4pd.v04

750 They should be read as such: Monte Carlo version, dataset number, generator, ?
751 name.

752 A.1.2 Background to signals

753 The same as the above though now with the filter as indicated by their name. The
754 second znunu sample has been generated with and center of mass energy at 8
755 TeV.

756 mc12.157539.sherpa_ct10_znunupt280d4pd.v05

757 mc12.157539.8tev_sherpa_ct10_znunupt280d4pd.v05

758 mc12.157536.sherpa_ct10_wtaunupt200d4pd.v05

759 mc12.157534.sherpa_ct10_wenupt200d4pd.v05

760 mc12.157535.sherpa_ct10_wmunupt200d4pd.v05

761 A.2 D5 signal processes

```

762 mc12.188408.madgraphpythia_auet2bcteq6l1_d5_dm50_ms10000_
763 qcut200d4pd.v06
764 mc12.188409.madgraphpythia_auet2bcteq6l1_d5_dm50_ms10000_
765 qcut400d4pd.v06
766 mc12.188410.madgraphpythia_auet2bcteq6l1_d5_dm50_ms10000_
767 qcut600d4pd.v06

768 mc12.188411.madgraphpythia_auet2bcteq6l1_d5_dm400_ms10000_
769 qcut200d4pd.v06
770 mc12.188412.madgraphpythia_auet2bcteq6l1_d5_dm400_ms10000_
771 qcut400d4pd.v06
772 mc12.188413.madgraphpythia_auet2bcteq6l1_d5_dm400_ms10000_
773 qcut600d4pd.v06

774 All signals should be read as such: Monte Carlo version, dataset number, genera-
775 tor, ?, name of operator, dark matter mass, default mass suppression scale,
776 qcut part. As discussed in reference
777 qcut means that the original data has been split into different parts depending on
778 the value of the lead jet pt.

```

779 A.3 Light vector mediator processes

```

780 mc12.188414.madgraphpythia_auet2bcteq6l1_dmv_dm50_mm100_w3_
781 qcut200d4pd.v06
782 mc12.188422.madgraphpythia_auet2bcteq6l1_dmv_dm50_mm100_w3_
783 qcut400d4pd.v06
784 mc12.188430.madgraphpythia_auet2bcteq6l1_dmv_dm50_mm100_w3_
785 qcut600d4pd.v06

786 mc12.188415.madgraphpythia_auet2bcteq6l1_dmv_dm50_mm300_w3_
787 qcut200d4pd.v06
788 mc12.188423.madgraphpythia_auet2bcteq6l1_dmv_dm50_mm300_w3_
789 qcut400d4pd.v06
790 mc12.188431.madgraphpythia_auet2bcteq6l1_dmv_dm50_mm300_w3_
791 qcut600d4pd.v06

792 mc12.188416.madgraphpythia_auet2bcteq6l1_dmv_dm50_mm500_w3_
793 qcut200d4pd.v06
794 mc12.188424.madgraphpythia_auet2bcteq6l1_dmv_dm50_mm500_w3_
795 qcut400d4pd.v06
796 mc12.188432.madgraphpythia_auet2bcteq6l1_dmv_dm50_mm500_w3_
797 qcut600d4pd.v06

798 mc12.188417.madgraphpythia_auet2bcteq6l1_dmv_dm50_mm1000_w3_
799 qcut200d4pd.v06
800 mc12.188425.madgraphpythia_auet2bcteq6l1_dmv_dm50_mm1000_w3_

```

```
801 qcut400d4pd.v06
802 mc12.188433.madgraphpythia_auet2bcteq6l1_dmv_dm50_mm1000_w3_
803 qcut600d4pd.v06
804 mc12.188418.madgraphpythia_auet2bcteq6l1_dmv_dm50_mm3000_w3_
805 qcut200d4pd.v06
806 mc12.188426.madgraphpythia_auet2bcteq6l1_dmv_dm50_mm3000_w3_
807 qcut400d4pd.v06
808 mc12.188434.madgraphpythia_auet2bcteq6l1_dmv_dm50_mm3000_w3_
809 qcut600d4pd.v06
810 mc12.188419.madgraphpythia_auet2bcteq6l1_dmv_dm50_mm6000_w3_
811 qcut200d4pd.v06
812 mc12.188427.madgraphpythia_auet2bcteq6l1_dmv_dm50_mm6000_w3_
813 qcut400d4pd.v06
814 mc12.188435.madgraphpythia_auet2bcteq6l1_dmv_dm50_mm6000_w3_
815 qcut600d4pd.v06
816 mc12.188420.madgraphpythia_auet2bcteq6l1_dmv_dm50_mm10000_w3_
817 qcut200d4pd.v06
818 mc12.188428.madgraphpythia_auet2bcteq6l1_dmv_dm50_mm10000_w3_
819 qcut400d4pd.v06
820 mc12.188436.madgraphpythia_auet2bcteq6l1_dmv_dm50_mm10000_w3_
821 qcut600d4pd.v06
822 mc12.188421.madgraphpythia_auet2bcteq6l1_dmv_dm50_mm15000_w3_
823 qcut200d4pd.v06
824 mc12.188429.madgraphpythia_auet2bcteq6l1_dmv_dm50_mm15000_w3_
825 qcut400d4pd.v06
826 mc12.188437.madgraphpythia_auet2bcteq6l1_dmv_dm50_mm15000_w3_
827 qcut600d4pd.v06
828 mc12.188438.madgraphpythia_auet2bcteq6l1_dmv_dm50_mm100_w8pi_
829 qcut200d4pd.v06
830 mc12.188446.madgraphpythia_auet2bcteq6l1_dmv_dm50_mm100_w8pi_
831 qcut400d4pd.v06
832 mc12.188454.madgraphpythia_auet2bcteq6l1_dmv_dm50_mm100_w8pi_
833 qcut600d4pd.v06
834 mc12.188439.madgraphpythia_auet2bcteq6l1_dmv_dm50_mm300_w8pi_
835 qcut200d4pd.v06
836 mc12.188447.madgraphpythia_auet2bcteq6l1_dmv_dm50_mm300_w8pi_
837 qcut400d4pd.v06
838 mc12.188455.madgraphpythia_auet2bcteq6l1_dmv_dm50_mm300_w8pi_
839 qcut600d4pd.v06
840 mc12.188440.madgraphpythia_auet2bcteq6l1_dmv_dm50_mm500_w8pi_
841 qcut200d4pd.v06
842 mc12.188448.madgraphpythia_auet2bcteq6l1_dmv_dm50_mm500_w8pi_
```

```
843 qcut400d4pd.v06
844 mc12.188456.madgraphpythia_auet2bcteq6l1_dmv_dm50_mm500_w8pi_
845 qcut600d4pd.v06

846 mc12.188441.madgraphpythia_auet2bcteq6l1_dmv_dm50_mm1000_w8pi_
847 qcut200d4pd.v06
848 mc12.188449.madgraphpythia_auet2bcteq6l1_dmv_dm50_mm1000_w8pi_
849 qcut400d4pd.v06
850 mc12.188457.madgraphpythia_auet2bcteq6l1_dmv_dm50_mm1000_w8pi_
851 qcut600d4pd.v06

852 mc12.188442.madgraphpythia_auet2bcteq6l1_dmv_dm50_mm3000_w8pi_
853 qcut200d4pd.v06
854 mc12.188450.madgraphpythia_auet2bcteq6l1_dmv_dm50_mm3000_w8pi_
855 qcut400d4pd.v06
856 mc12.188458.madgraphpythia_auet2bcteq6l1_dmv_dm50_mm3000_w8pi_
857 qcut600d4pd.v06

858 mc12.188444.madgraphpythia_auet2bcteq6l1_dmv_dm50_mm10000_w8pi_
859 qcut200d4pd.v06
860 mc12.188452.madgraphpythia_auet2bcteq6l1_dmv_dm50_mm10000_w8pi_
861 qcut400d4pd.v06
862 mc12.188460.madgraphpythia_auet2bcteq6l1_dmv_dm50_mm10000_w8pi_
863 qcut600d4pd.v06

864 mc12.188445.madgraphpythia_auet2bcteq6l1_dmv_dm50_mm15000_w8pi_
865 qcut200d4pd.v06
866 mc12.188453.madgraphpythia_auet2bcteq6l1_dmv_dm50_mm15000_w8pi_
867 qcut400d4pd.v06
868 mc12.188461.madgraphpythia_auet2bcteq6l1_dmv_dm50_mm15000_w8pi_
869 qcut600d4pd.v06

870 mc12.188462.madgraphpythia_auet2bcteq6l1_dmv_dm400_mm500_w3_
871 qcut200d4pd.v06
872 mc12.188468.madgraphpythia_auet2bcteq6l1_dmv_dm400_mm500_w3_
873 qcut400d4pd.v06
874 mc12.188474.madgraphpythia_auet2bcteq6l1_dmv_dm400_mm500_w3_
875 qcut600d4pd.v06

876 mc12.188463.madgraphpythia_auet2bcteq6l1_dmv_dm400_mm1000_w3_
877 qcut200d4pd.v06
878 mc12.188469.madgraphpythia_auet2bcteq6l1_dmv_dm400_mm1000_w3_
879 qcut400d4pd.v06
880 mc12.188475.madgraphpythia_auet2bcteq6l1_dmv_dm400_mm1000_w3_
881 qcut600d4pd.v06

882 mc12.188464.madgraphpythia_auet2bcteq6l1_dmv_dm400_mm3000_w3_
883 qcut200d4pd.v06
884 mc12.188470.madgraphpythia_auet2bcteq6l1_dmv_dm400_mm3000_w3_
```

```
885 qcut400d4pd.v06
886 mc12.188476.madgraphpythia_auet2bcteq6l1_dmv_dm400_mm3000_w3_
887 qcut600d4pd.v06
888 mc12.188465.madgraphpythia_auet2bcteq6l1_dmv_dm400_mm6000_w3_
889 qcut200d4pd.v06
890 mc12.188471.madgraphpythia_auet2bcteq6l1_dmv_dm400_mm6000_w3_
891 qcut400d4pd.v06
892 mc12.188477.madgraphpythia_auet2bcteq6l1_dmv_dm400_mm6000_w3_
893 qcut600d4pd.v06
894 mc12.188466.madgraphpythia_auet2bcteq6l1_dmv_dm400_mm10000_w3_
895 qcut200d4pd.v06
896 mc12.188472.madgraphpythia_auet2bcteq6l1_dmv_dm400_mm10000_w3_
897 qcut400d4pd.v06
898 mc12.188478.madgraphpythia_auet2bcteq6l1_dmv_dm400_mm10000_w3_
899 qcut600d4pd.v06
900 mc12.188467.madgraphpythia_auet2bcteq6l1_dmv_dm400_mm15000_w3_
901 qcut200d4pd.v06
902 mc12.188473.madgraphpythia_auet2bcteq6l1_dmv_dm400_mm15000_w3_
903 qcut400d4pd.v06
904 mc12.188479.madgraphpythia_auet2bcteq6l1_dmv_dm400_mm15000_w3_
905 qcut600d4pd.v06
906 mc12.188480.madgraphpythia_auet2bcteq6l1_dmv_dm400_mm500_w8pi_
907 qcut200d4pd.v06
908 mc12.188486.madgraphpythia_auet2bcteq6l1_dmv_dm400_mm500_w8pi_
909 qcut400d4pd.v06
910 mc12.188492.madgraphpythia_auet2bcteq6l1_dmv_dm400_mm500_w8pi_
911 qcut600d4pd.v06
912 mc12.188481.madgraphpythia_auet2bcteq6l1_dmv_dm400_mm1000_w8pi_
913 qcut200d4pd.v06
914 mc12.188487.madgraphpythia_auet2bcteq6l1_dmv_dm400_mm1000_w8pi_
915 qcut400d4pd.v06
916 mc12.188493.madgraphpythia_auet2bcteq6l1_dmv_dm400_mm1000_w8pi_
917 qcut600d4pd.v06
918 mc12.188482.madgraphpythia_auet2bcteq6l1_dmv_dm400_mm3000_w8pi_
919 qcut200d4pd.v06
920 mc12.188488.madgraphpythia_auet2bcteq6l1_dmv_dm400_mm3000_w8pi_
921 qcut400d4pd.v06
922 mc12.188494.madgraphpythia_auet2bcteq6l1_dmv_dm400_mm3000_w8pi_
923 qcut600d4pd.v06
924 mc12.188483.madgraphpythia_auet2bcteq6l1_dmv_dm400_mm6000_w8pi_
925 qcut200d4pd.v06
926 mc12.188489.madgraphpythia_auet2bcteq6l1_dmv_dm400_mm6000_w8pi_
```

```
927 qcut400d4pd.v06
928 mc12.188495.madgraphpythia_auet2bcteq6l1_dmv_dm400_mm6000_w8pi_
929 qcut600d4pd.v06
930 mc12.188484.madgraphpythia_auet2bcteq6l1_dmv_dm400_mm10000_w8pi_
931 qcut200d4pd.v06
932 mc12.188490.madgraphpythia_auet2bcteq6l1_dmv_dm400_mm10000_w8pi_
933 qcut400d4pd.v06
934 mc12.188496.madgraphpythia_auet2bcteq6l1_dmv_dm400_mm10000_w8pi_
935 qcut600d4pd.v06
936 mc12.188485.madgraphpythia_auet2bcteq6l1_dmv_dm400_mm15000_w8pi_
937 qcut200d4pd.v06
938 mc12.188491.madgraphpythia_auet2bcteq6l1_dmv_dm400_mm15000_w8pi_
939 qcut400d4pd.v06
940 mc12.188497.madgraphpythia_auet2bcteq6l1_dmv_dm400_mm15000_w8pi_
941 qcut600d4pd.v06
```

Bibliography

- [1] Collaboration ATLAS. Letter of Intent for the Phase-II Upgrade of the ATLAS Experiment. Dec 2012. URL <https://cds.cern.ch/record/1502664/>. Cited on pages 1, 17, 25, and 27.
- [2] B.H. Bransden and C.J. Joachain. *Quantum mechanics*. Pearson Education, second edition, 2000. Cited on page 3.
- [3] Sven-Patrik Hallsjö. Covering the sphere with noncontextuality inequalities. Bachelor's thesis, Linköping University, The Institute of Technology, 2013. URL [http://urn.kb.se/resolve?urn=urn:nbn:se:liu:diva-103663](http://urn.kb.se/resolve?urn=urn:nbn:se:liu.diva-103663). Cited on page 3.
- [4] A. Zee. *Quantum Field Theory in a Nutshell*. Princeton University Press, illustrated edition edition, March 2003. ISBN 0691010196. Cited on pages 3, 6, and 7.
- [5] Herbert Goldstein, Charles P. Poole, and John L. Safko. *Classical Mechanics (3rd Edition)*. Addison-Wesley, 3 edition, June 2001. ISBN 0201657023. Cited on page 3.
- [6] W. E. Burcham and M. Jobes. *Nuclear and Particle Physics*. Pearson education, second edition, 1995. Cited on page 4.
- [7] The ATLAS Collaboration. Observation of a new particle in the search for the Standard Model Higgs boson with the ATLAS detector at the LHC. *Phys. Lett. B*, 716(arXiv:1207.7214). CERN-PH-EP-2012-218):1–29. 39 p, Aug 2012. Cited on page 4.
- [8] Standard model of elementary particles. http://en.wikipedia.org/wiki/File:Standard_Model_of_Elementary_Particles.svg, 2014. Accessed: 2014-03-24. Cited on page 4.
- [9] G. Jungman, M. Kamionkowski, and K. Griest. Supersymmetric dark matter. *Physics Reports*, 267:195–373, March 1996. doi: 10.1016/0370-1573(95)00058-5. Cited on pages 4 and 5.

- 971 [10] NASA. NASA's solar system exploration: the planets: orbits and
972 physical characteristics. [https://solarsystem.nasa.gov/planets/](https://solarsystem.nasa.gov/planets/charchart.cfm)
973 charchart.cfm, 2014. Accessed: 2014-03-21. Cited on page 6.
- 974 [11] T. S. van Albada, J. N. Bahcall, K. Begeman, and R. Sancisi. Distribution
975 of dark matter in the spiral galaxy NGC 3198. *Astrophysical Journal*, 295:
976 305–313, August 1985. doi: 10.1086/163375. Cited on page 6.
- 977 [12] Jessica Goodman, Masahiro Ibe, Arvind Rajaraman, William Shepherd,
978 Tim M.P. Tait, et al. Constraints on Light Majorana dark Matter from Colliders.
979 *Phys.Lett.*, B695:185–188, 2011. doi: 10.1016/j.physletb.2010.11.009.
980 Cited on pages 5 and 7.
- 981 [13] ATLAS Collaboration. Search for dark matter candidates and large extra di-
982 mensions in events with a jet and missing transverse momentum with the at-
983 las detector. *J. High Energy Phys.*, 04(arXiv:1210.4491. CERN-PH-EP-2012-
984 210):075. 58 p, October 2012. URL [http://cds.cern.ch/record/](http://cds.cern.ch/record/1485031)
985 1485031. Cited on pages 5, 8, and 9.
- 986 [14] J. Goodman, M. Ibe, A. Rajaraman, W. Shepherd, T. M. P. Tait, and H.-B. Yu.
987 Constraints on dark matter from colliders. *Phys.Rev.D82:116010,2010*, 82
988 (11):116010, December 2010. doi: 10.1103/PhysRevD.82.116010. Cited on
989 page 7.
- 990 [15] ATLAS. Atlas luminosity public results. <https://twiki.cern.ch/twiki/bin/view/AtlasPublic/LuminosityPublicResults>, 2013.
991 Accessed: 2014-03-06. Cited on page 10.
- 992 [16] AC Team. The four main LHC experiments, Jun 1999. URL <http://cds.cern.ch/record/40525>. Cited on page 10.
- 993 [17] Werner Herr and B Muratori. Concept of luminosity. 2006. URL <http://cds.cern.ch/record/941318/>. Cited on page 11.
- 994 [18] The ATLAS Collaboration. The atlas experiment at the cern large hadron col-
995 linder. *Journal of Instrumentation*, 3(08):S08003. 437 p, 2008. URL <https://cdsweb.cern.ch/record/1129811/>. Cited on pages 11 and 12.
- 996 [19] Joao Pequenao. Computer generated image of the whole ATLAS detector,
997 Mar 2008. URL <http://cds.cern.ch/record/1095924>. Cited on page
998 12.
- 999 [20] ATLAS Collaboration. Event display for one of the monojet candidates in
1000 the data. The event has a jet with $\text{pt} = 602 \text{ GeV}$ at $\eta = -1$ and $\phi =$
1001 2.6 , $\text{MET} = 523 \text{ GeV}$, and no additional jet with $\text{pt}_{\text{jet}} > 30 \text{ GeV}$ in the fi-
1002 nal state.. [https://atlas.web.cern.ch/Atlas/GROUPS/PHYSICS/](https://atlas.web.cern.ch/Atlas/GROUPS/PHYSICS/CONFNOTES/ATLAS-CONF-2011-096/fig_08.png)
1003 CONFNOTES/ATLAS-CONF-2011-096/fig_08.png, 2011. Accessed:
1004 2014-03-28. Cited on page 13.
- 1005 [21] ATLAS Collaboration. Physics at a High-Luminosity LHC with ATLAS. Jul
1006

- 1010 2013. URL <https://cds.cern.ch/record/1564937>. Cited on page
1011 15.
- 1012 [22] J. Alwall, M. Herquet, F. Maltoni, O. Mattelaer, and T. Stelzer. MadGraph
1013 5: going beyond. *Journal of High Energy Physics*, 6:128, June 2011. doi:
1014 10.1007/JHEP06(2011)128. Cited on page 15.
- 1015 [23] Torbjörn Sjöstrand, Stephen Mrenna, and Peter Skands. A brief introduc-
1016 tion to {PYTHIA} 8.1. *Computer Physics Communications*, 178(11):852 –
1017 867, 2008. ISSN 0010-4655. doi: [http://dx.doi.org/10.1016/j.cpc.2008.
1018 01.036](http://dx.doi.org/10.1016/j.cpc.2008.01.036). URL [http://www.sciencedirect.com/science/article/
1019 pii/S0010465508000441](http://www.sciencedirect.com/science/article/pii/S0010465508000441). Cited on page 15.
- 1020 [24] The ROOT Team. Root. <http://root.cern.ch/drupal/>, 2014. Ac-
1021 cessed: 2014-03-28. Cited on page 15.
- 1022 [25] ATLAS Collaboration. Performance assumptions for an upgraded ATLAS
1023 detector at a High-Luminosity LHC. Mar 2013. URL [https://cds.cern.
1024 ch/record/1527529/](https://cds.cern.ch/record/1527529/). Cited on pages 17, 19, 25, 26, and 27.
- 1025 [26] ATLAS Collaboration. Electron performance measurements with the ATLAS
1026 detector using the 2010 LHC proton-proton collision data. *Eur. Phys. J. C*,
1027 72(arXiv:1110.3174. CERN-PH-EP-2011-117):1909. 45 p, Oct 2011. Com-
1028 ments: 33 pages plus author list (45 pages total), 24 figures, 12 tables, sub-
1029 mitted to Eur. Phys. J. C. Cited on pages 25 and 27.
- 1030 [27] ATLAS Collaboration. Search for New Phenomena in Monojet plus Missing
1031 Transverse Momentum Final States using 10fb-1 of pp Collisions at $\sqrt{s}=8$
1032 TeV with the ATLAS detector at the LHC. Nov 2012. URL <http://cds.cern.ch/record/1493486/>. Cited on pages 30 and 31.
- 1033 [28] Donald Duck. The history of automatic control. *Duckburg Journal of Sci-
1034 ence*, 106(3):345–401, 2005. Cited on page 36.
- 1035



1037 Upphovsrätt

1038 Detta dokument hålls tillgängligt på Internet — eller dess framtida ersättare —
 1039 under 25 år från publiceringsdatum under förutsättning att inga extraordinära
 1040 omständigheter uppstår.

1041 Tillgång till dokumentet innebär tillstånd för var och en att läsa, ladda ner,
 1042 skriva ut enstaka kopior för enskilt bruk och att använda det oförändrat för icke-
 1043 kommersiell forskning och för undervisning. Överföring av upphovsrätten vid
 1044 en senare tidpunkt kan inte upphäva detta tillstånd. All annan användning av
 1045 dokumentet kräver upphovsmannens medgivande. För att garantera äktheten,
 1046 säkerheten och tillgängligheten finns det lösningar av teknisk och administrativ
 1047 art.

1048 Upphovsmannens ideella rätt innehåller rätt att bli nämnd som upphovsman
 1049 i den omfattning som god sed kräver vid användning av dokumentet på ovan
 1050 beskrivna sätt samt skydd mot att dokumentet ändras eller presenteras i sådan
 1051 form eller i sådant sammanhang som är kränkande för upphovsmannens litterära
 1052 eller konstnärliga anseende eller egenart.

1053 För ytterligare information om Linköping University Electronic Press se för-
 1054 lagets hemsida <http://www.ep.liu.se/>

1055 Copyright

1056 The publishers will keep this document online on the Internet — or its possi-
 1057 ble replacement — for a period of 25 years from the date of publication barring
 1058 exceptional circumstances.

1059 The online availability of the document implies a permanent permission for
 1060 anyone to read, to download, to print out single copies for his/her own use and
 1061 to use it unchanged for any non-commercial research and educational purpose.
 1062 Subsequent transfers of copyright cannot revoke this permission. All other uses
 1063 of the document are conditional on the consent of the copyright owner. The
 1064 publisher has taken technical and administrative measures to assure authenticity,
 1065 security and accessibility.

1066 According to intellectual property law the author has the right to be men-
 1067 tioned when his/her work is accessed as described above and to be protected
 1068 against infringement.

1069 For additional information about the Linköping University Electronic Press
 1070 and its procedures for publication and for assurance of document integrity, please
 1071 refer to its www home page: <http://www.ep.liu.se/>